Molecular Medicine

Peroxisome Proliferator-Activated Receptor γ 2 Modulates Late-Pregnancy Homeostatic Metabolic Adaptations

Yurena Vivas,[1] Monica Díez-Hochleitner,[1,2] Adriana Izquierdo-Lahuerta,[1] Patricia Corrales,[1] Daniel Horrillo,[1] Ismael Velasco,[1] Cristina Martínez-García,[1] Mark Campbell,[3] Julio Sevillano,[2] Mercedes Ricote,[4] Manuel Ros,[1] Maria Pilar Ramos,[2] and Gema Medina-Gomez[1,5]

[1]Department of Basic Sciences of Health, Area of Biochemistry and Molecular Biology, University Rey Juan Carlos, Madrid, Spain; [2]Faculty of Pharmacy, University CEU San Pablo, Madrid, Spain; [3]Metabolic Research Laboratories, Institute of Metabolic Science, Addenbrooke's Hospital, University of Cambridge, UK; [4]National Center of Cardiovascular Research Carlos III, Madrid, Spain; and [5]Research Unit, University Rey Juan Carlos-Institute of Biomedical Research "Alberto Sols" (CSIC)

Pregnancy requires adaptation of maternal energy metabolism, including expansion and functional modifications of adipose tissue. Insulin resistance (IR), predominantly during late gestation, is a physiological metabolic adaptation that serves to support the metabolic demands of fetal growth. The molecular mechanisms underlying these adaptations are not fully understood and may contribute to gestational diabetes mellitus. Peroxisome proliferator-activated receptor γ (PPARγ) controls adipogenesis, glucose and lipid metabolism and insulin sensitivity. The PPARγ2 isoform is mainly expressed in adipocytes and is thus likely to contribute to adipose tissue adaptation during late pregnancy. In the present study, we investigated the contribution of PPARγ2 to the metabolic adaptations occurring during the late phase of pregnancy in the context of IR. Using a model of late pregnancy in PPARγ2 knockout (KO) mice, we found that deletion of PPARγ2 exacerbated IR in association with lower serum adiponectin levels, increased body weight and enhanced lipid accumulation in the liver. Lack of PPARγ2 provoked changes in the distribution of fat mass and preferentially prevented expansion of the perigonadal depot while at the same time exacerbating inflammation. Pregnant PPARγ2KO mice presented adipose tissue depot-dependent decreased expression of genes involved in lipid metabolism. Collectively, these data indicate that PPARγ2 is essential in promoting healthy adipose tissue expansion and immune and metabolic functionality during pregnancy, contributing to the physiological adaptations that lead gestation to term.

INTRODUCTION

A successful pregnancy requires adaptations of maternal energy metabolism, including adipose tissue expansion and changes in functionality. Two distinct metabolic phases can be identified during pregnancy: a predominantly anabolic phase followed by a predominantly catabolic phase.

The second phase is characterized by lipolysis and insulin resistance (IR) during late stages of pregnancy, which facilitates mobilization of fuel to support the increased energy demands of late fetal growth (1).

Development of IR in late gestation may induce excessive metabolic stress in the mother, ultimately leading to gestational diabetes mellitus (GDM). The molecular mechanisms promoting gestational IR are not fully understood. There is evidence for impairment in insulin signaling pathways, in both muscle and adipose tissue (2,3). Hormonal changes, inflammation and/or an increase in circulating triglycerides may also contribute to these alterations (4). In addition, a decrease in adiponectin levels has been detected during pregnancy, suggesting a potential link with insulin sensitivity (3).

During early pregnancy, as in obesity, mechanisms leading to energy storage and adipose tissue expansion are activated. However, the fact that some individuals with morbid obesity maintain a healthy metabolism (5) in contrast to the inappropriate excessive IR observed in overweight individuals with central

Address correspondence to Gema Medina-Gomez, Department of Basic Sciences of Health, Area of Biochemistry and Molecular Biology, University Rey Juan Carlos Faculty of Sciences of Health, Avda. de Atenas s/n, 28922 Alcorcón-Madrid, Spain. Phone: + 34 91 4888632; Fax: + 34 91 4888831; E-mail: gema.medina@urjc.es

fat distribution (6–8) suggests that the absolute amount of fat is not the main determinant of the degree of IR. Other factors, such as fat localization or the degree of inflammation (9,10), may also be relevant.

The nuclear receptor peroxisome proliferator-activated receptor γ (PPARγ) is a ligand-activated transcription factor involved in adipogenesis and glucose-lipid metabolism. Of the two known PPARγ isoforms, PPARγ1 is widely distributed in tissues, whereas PPARγ2 is more specific to adipose tissues. We previously generated a mouse model of PPARγ2 deficiency (PPγ2KO) (11), which is insulin resistant and presents adipose tissue dysfunction, particularly when challenged with positive energy balance (12). Moreover, PPARγ2 seems to be important for pancreatic β-cell mass adaptation in murine models of the metabolic syndrome (13,14). We previously showed that PPARγ agonists reverse IR associated with late pregnancy in rats (3), and there is evidence that *PPARγ* expression in adipose tissue in obese women with GDM is lower than in obese women with an uncomplicated pregnancy (15). Thus we hypothesize that PPARγ may be an important contributor to the metabolic adaptations required in adipose tissue during pregnancy and may regulate insulin sensitivity. Here we studied the role of PPARγ2 in the metabolic adaptations associated with the last phase of pregnancy in mice when a state of IR is established (16).

MATERIALS AND METHODS

Ethical Approval and Animal Care

Animals were housed in a temperature-controlled room with a 12 h light/dark cycle. Food and water were available *ad libitum* unless otherwise noted. Mice were fed a standard chow diet (13% of calories derived from fat; Envigo). Animal protocols were approved by the Rey Juan Carlos University ethics committee.

Pregnancy Studies and Serum Biochemistry

Female wild-type (WT-C) and PPARγ2 knockout (PPγ2KO-C) mice (3 months of age; mixed background 129Sv/C57BL6) (14) were crossed with WT males.

Serum levels of progesterone were measured with commercial ELISA kits (Progesterone EIA kit; Cayman Chemical). Serum insulin, adipokines and cytokines were determined with Bio-Plex assays (Bio-Plex Pro™ Diabetes Assays, Bio-Rad). Commercial enzymatic assay kits were used for determination of free fatty acids (HR series NEFA-HR(2); Wako) and total triacylglycerides (Spinreact).

Histology and Immunohistochemistry

Samples of pancreas and white adipose tissue (WAT) were fixed in Bouin's solution, gradually dehydrated and embedded in paraffin, cut to 4 μm, and stained with Harris hematoxylin (Sigma Chemical) or incubated with anti-MCP-1 (Santa Cruz Biotechnology), anti-insulin or anti-CHOP protein antibodies (Santa Cruz Biotechnology).

The area of islets from pancreas tail sections was quantified in four nonconsecutive slides per animal (n = 4 animals/group), leaving at least 80 μm between consecutive slides. In total, three to seven different regions were measured.

Glucose and Insulin Tolerance Tests

Glucose tolerance test (GTT) was performed in the four experimental groups at d 15 (D15) of gestation, and insulin tolerance test (ITT) was performed only in pregnant groups at D16 as previously described (12).

Insulin Stimulation

Mice that had fasted for 16 h were injected intraperitoneally with human insulin (Actrapid, 10 U/kg body weight; Novo Nordisk) or saline (NaCl, 0.9%). Adipose tissue and muscle samples were collected five minutes after injection for protein extraction.

RNA Extraction and Real-Time Quantitative Polymerase Chain Reaction (RT-PCR)

RNA extraction and quantitative RT-PCR were performed as reported (14,17). The input value of the gene of interest was standardized to a best housekeeper gene calculated using three different genes, 18S rRNA, *β2-microglobulin* and *β*-actin mRNA, and the BestKeeper software tool (18). The primers used are listed in Supplementary Table S1.

Western Blot Analysis

Protein lysates from tissues were subjected to sodium dodecyl sulfate polyacrylamide gel electrophoresis (SDS-PAGE) (7.5% or 10% polyacrylamide) and probed with the following antibodies (17): phosphorylated-Ser473-Akt (Cell Signaling Technology); total Akt, phosphorylated-Tyr1162/1136-β-insulin receptor and total β-insulin receptor (all from Santa Cruz Biotechnology); PPARγ (E-8; Santa Cruz Biotechnology); and HSL total and ATGL (both from Cell Signaling Technology). Membranes were stripped and reprobed with rabbit anti-β-actin antibody (Sigma-Aldrich) to correct for differences in loading. Protein band density was measured using ImageJ v1.45 software (National Institutes of Health). The amount of protein in control conditions was assigned a relative value of 100%.

Liver and Adipose Tissue Total Lipid Content

Total lipids were extracted and determined from samples (100 mg tissue) using the method of Folch *et al.* (19) with modifications (20).

Statistical Analysis

All results are presented as the mean ± standard error of the mean (SEM). The data were analyzed using SPSS software (IBM). Analysis of variance (ANOVA) followed by *post hoc* Bonferroni test was used in statistical comparisons between four groups. Statistical comparisons between two groups were performed using Student *t* test. When data were not normally distributed, the nonparametric

Kruskal-Wallis or Mann Whitney-U test was applied. The significance level was set at $p ≤ .05$.

All supplementary materials are available online at www.molmed.org.

RESULTS

Gene Expression Analysis of PPARγ Isoforms and Their Target Genes in WAT Depots During the Late Stages of a Healthy Pregnancy

Healthy pregnant (WT-P) mice increased their body weight by 70% during pregnancy (Figure 1A and Table 1). Approximately two-thirds of the weight gain was associated with the fetus and placenta; the remaining one-third resulted from the increase in the weight of the maternal carcass. Food intake increased progressively from mid-pregnancy (D10), and the overall food intake of the pregnant animals increased by 16% (Figure 1B).

We analyzed the expression of both PPARγ isoforms together with genes involved in lipid metabolism in different WAT depots at late pregnancy, when metabolic changes are associated with increased lipolysis and IR. *PPARγ1* and, to a lesser extent, *PPARγ2* showed a tendency toward higher mRNA expression in perigonadal fat in WT-P mice than in WT-C mice at late gestation (Figure 2A). Consistent with this, protein levels of PPARγ1 were unchanged and a nonsignificant increase in PPARγ2 protein was found in WT-P mice (Figure 2B). *Adiponectin, leptin, adipsin* and *aP2* mRNA expression mirrored *PPARγ1* and *PPARγ2* expression in the perigonadal depot (Figure 2A). The expression levels of genes implicated in fatty acid synthesis, such as *Fas, Scd1* and *Acc*, were unchanged relative to their levels in WT-C mice (Figure 3A). Likewise, the mRNA expression of enzymes implicated in synthesis of triacyl-glycerides (*Dgat2*) and lipid accumulation (*Lpl*) were unchanged in perigonadal WAT during pregnancy. However, genes related to lipolysis, such as *Atgl, Hsl* and *G0s2*, exhibited a tendency toward

higher mRNA expression during late pregnancy (Figure 3A). Protein expression of ATGL and HSL was similar to mRNA expression in perigonadal WAT during late pregnancy (Figure 3B).

In the subcutaneous depot of WT-C animals, mRNA expression of *PPARγ2* significantly decreased during late pregnancy, whereas *PPARγ1* expression remained unchanged (Figure 2C). Protein levels of both isoforms showed a similar pattern to that of mRNA expression (Figure 2D). Moreover, mRNA expression of *PPARα, adiponectin, adipsin* and *aP2* in subcutaneous WAT was lower in WT-P mice than in WT-C mice (Figure 2C). Similarly *Fas, Scd1, Dgat2* and *Lpl* mRNA levels were lower in WT-P mice than in WT-C mice. Lipolytic gene expression in the subcutaneous depot was lower at the end of pregnancy in WT-P mice than in WT-C mice, and was clearly different to that found in the perigonadal depot (compare Figures 3A and C). Although not significant, levels of ATGL protein in subcutaneous WAT were also lower in WT-P mice than in WT-C mice (Figure 3D).

Deletion of PPARγ2 Leads to Increased Body Weight in Pregnant Mice During Late Gestation

Growth rates of PPγ2KO-P and WT-P mice were similar until d 16 (D16) of pregnancy (Figure 1A). From this point onward, an unexpected and significant increase in the body weight of PPγ2KO-P mice was maintained until D18. The difference in body weight remained after removing the conceptus (Table 1). No differences in placental or fetal weight, or in the number of fetuses in each litter, were observed between pregnant genotypes. Food intake was not different between the two groups; however, discrete and significant increases of food intake were observed in PPγ2KO-P mice at D3, D4 and D11 (Figure 1B). No differences in body weight were found between genotypes of nonpregnant mice, as previously reported by us (WT-C = 22.59 ± 0.51g; PPγ2KO-C = 23.85 ± 0.55 g) (12).

The increased body weight of PPγ2KO-P mice during the last term of gestation was associated with increased liver and pancreas weight (Table 1). Of note, despite being heavier, the weight of perigonadal fat was significantly lower in PPγ2KO-P mice than in WT-P mice (Table 1). By contrast, no differences were found in the weight of inguinal subcutaneous fat or scapular brown fat between the PPγ2KO-P and WT-P groups.

Deletion of PPARγ2 Is Associated with More Severe Insulin Resistance (IR) During Late Pregnancy

We hypothesized that PPARγ2 might contribute to the regulation of insulin sensitivity within a physiological range during pregnancy, and therefore might prevent pregnancy-related complications. At D18, fed glucose levels were significantly lower in WT-P mice than in WT controls, as frequently occurs during the last stage of gestation (Table 2). Accordingly, insulin levels showed a tendency to be higher in WT-P mice than in WT-C mice (Table 2). However, whereas no differences in glycemia were observed between PPγ2KO-P and PPγ2KO-C mice, fed levels of insulin were significantly higher in PPγ2KO-P mice than in nonpregnant controls and WT-P mice. Furthermore, adiponectin levels were strongly decreased in the PPγ2KO-P group with respect to all the experimental groups. Although circulating leptin was significantly increased at d 18 (D 18) in pregnant animals, no differences were detected between the PPγ2KO-P and WT-P groups. The leptin/adiponectin ratio, a potential biomarker of IR (21), was 4.4-fold higher in PPγ2KO-P mice than in WT-P mice (Table 2). The levels of triacylglycerides (TGs) were significantly higher in PPγ2KO-P mice than in PPγ2KO-C mice, and we observed a tendency toward higher fed TGs and fasting free fatty acids in the PPγ2KO-P compared to the WT-P group (Table 2).

We next examined whole-body insulin sensitivity. GTTs performed at D15 revealed significantly higher glucose intolerance in WT-P mice than in WT-C
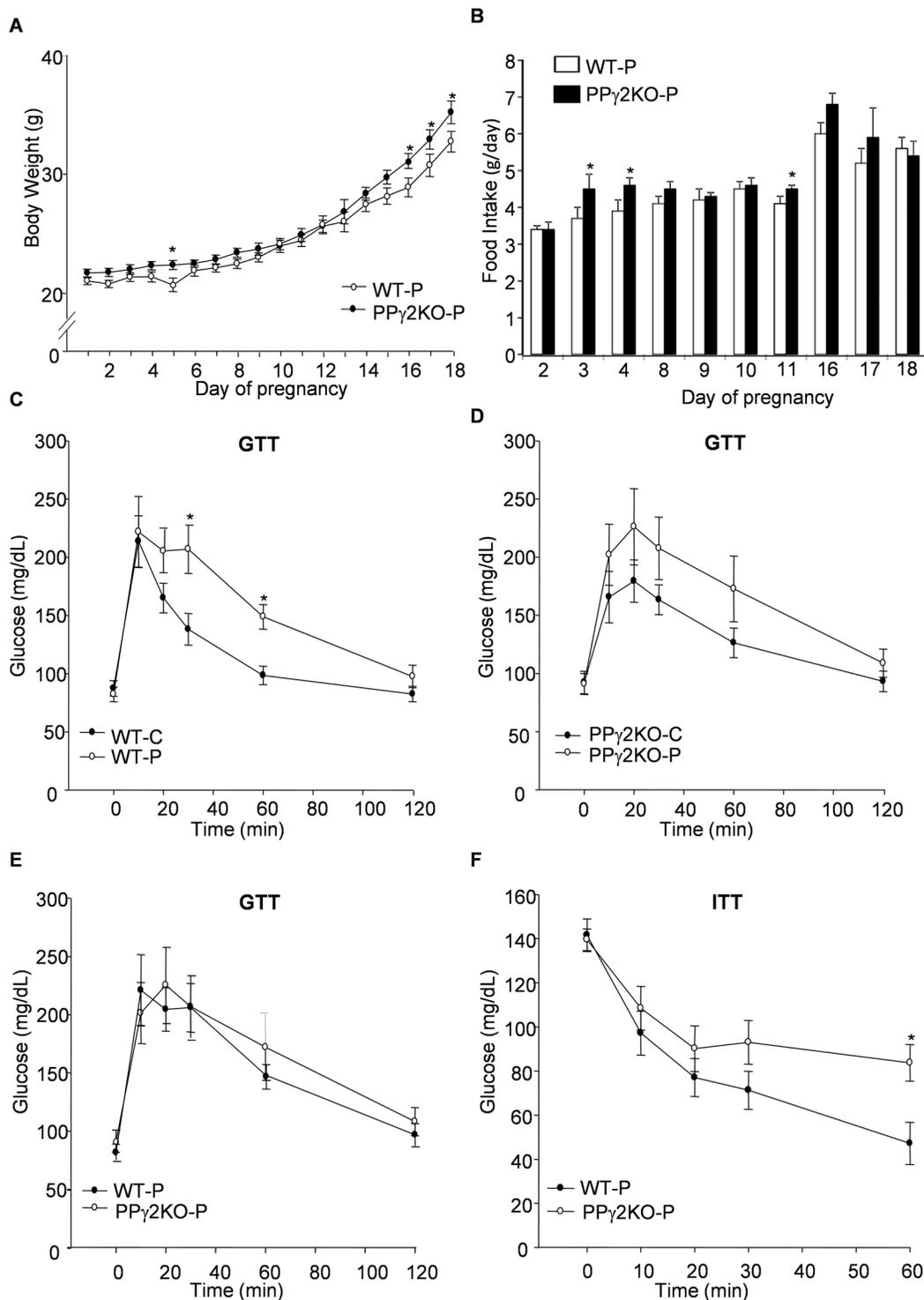
Figure 1. Alteration in body weight, food intake and insulin sensitivity in PPARγ2KO mice during pregnancy. (A) Evolution of body weight in pregnant mice with deletion of PPARγ2 (PPγ2KO-P) and in corresponding pregnant WT (WT-P) animals. (B) Changes in food intake during pregnancy. Food intake was measured every 24 h. Data from the first, second and third phase of pregnancy are shown. (C) GTT curves from nonpregnant and pregnant WT mice, (D) from nonpregnant and pregnant PPγ2KO mice and (E) from pregnant WT and PPγ2KO mice. All mice were at d 15 of gestation. (F) ITT curves from pregnant WT and PPγ2KO mice at d 16 of gestation. Data are expressed as mean ± SEM (A, B: n = 10–15 animals/group; C–F: n = 9–11 animals/group). *$p \leq .05$.

Table 1. Body weight, weight of fetuses, body mass distribution and tissue lipid content during pregnancy in WT and PPARγ2KO mice.

	WT-P	PPγ2KO-P
Total body weight (g)	32.50 ± 1.34	37.62 ± 1.77*
Body weight without conceptus (g)	25.25 ± 0.60	30.81 ± 0.99***
Placenta (g)	0.11 ± 0.01	0.11 ± 0.01
Fetus (g)	0.93 ± 0.07	0.92 ± 0.04
Litter size (number)	6.44 ± 0.80	6.66 ± 1.12
Pancreas (g)	0.38 ± 0.02	0.45 ± 0.02*
Liver (g)	1.51 ± 0.04	1.73 ± 0.05**
Hepatic lipid content (mg/g)	51.50 ± 1.40	58.50 ± 1.70*
Perigonadal adipose tissue (g)	0.21 ± 0.02	0.14 ± 0.02*
Perigonadal adipose tissue lipid content (mg/g)	0.79 ± 0.025	0.77 ± 0.035
Subcutaneous adipose tissue (g)	0.49 ± 0.02	0.52 ± 0.04
Subcutaneous adipose tissue lipid content (mg/g)	0.61 ± 0.030	0.64 ± 0.044
Brown adipose tissue (g)	0.11 ± 0.01	0.13 ± 0.01

Data are presented as mean ± SEM (n = 8–10 animals/group). *$p \leq .05$; **$p \leq .01$ ***$p \leq .001$, PPγ2KO-P versus WT-P. P: d 18 pregnant mice.

mice, as shown by slower clearance of glucose (Figure 1C). A similar but non-significant tendency was observed in PPγ2KO-P mice relative to PPγ2KO-C mice (Figure 1D). No differences in glucose tolerance were observed between the two pregnant genotypes (Figure 1E). Nevertheless, a higher degree of IR was observed in PPγ2KO-P mice relative to WT-P mice, as shown by impaired glucose disposal in the ITT at D16 (Figure 1F). To investigate whether the higher peripheral IR observed in PPγ2KO-P mice was associated with altered insulin signaling in WAT tissue, we measured phosphorylation of the major insulin signaling protein Akt in subcutaneous and perigonadal WAT depots after insulin injection. As expected, insulin induced phosphorylation of 473-Ser Akt in both fat depots of WT-C mice; however, this response was lost in all pregnant mice irrespective of fat depot or genotype (Supplementary Figure S1A and S1B). We also investigated insulin signaling in the muscle depot. Basal levels of β-insulin receptor phosphorylation were appreciably higher in PPγ2KO-P mice than in the other groups (Supplementary Figure S1C). Whereas WT-P mice showed a tendency for β-insulin receptor phosphorylation, no stimulation of signaling was observed in muscle from PPγ2KO-P

mice (Supplementary Figure S1C), suggesting a lower response to insulin.

PPARγ2 Differentially Regulates Fat Storage and Mobilization Genes in Perigonadal and Subcutaneous WAT Depots During Pregnancy

Histological analysis of subcutaneous and perigonadal WAT did not reveal any obvious differences in morphology or size of adipocytes between PPγ2KO-P and WT-P mice (Supplementary Figure S2). Although the total lipid content was lower in subcutaneous than perigonadal WAT in pregnant animals, no significant differences were found between both genotypes in either WAT depot (Table 1).

Regarding expression in the subcutaneous depot, mRNA and protein levels of PPARγ1 were significantly lower in PPγ2KO-P mice than in the other groups (Figures 2C and D). *Adipsin* mRNA expression significantly decreased during pregnancy, and levels were considerably lower in PPγ2KO-P mice than in WT-P mice. Moreover, lipogenesis-related gene expression was significantly lower in PPγ2KO-P mice than in the other groups. Pro-oxidative genes, such as *PPARα*, also showed lower mRNA expression in PPγ2KO-P, whereas *PPARδ* mRNA expression remained unchanged (Figure 2C). The mRNA levels of *Atgl*

and *Hsl* were decreased by pregnancy in both genotypes, but their levels were significantly lower in PPγ2KO-P mice than in WT-P mice (Figure 3C). The same trend, albeit not significant, was found for ATGL and HSL protein levels (Figure 3D).

In the perigonadal depot there was a similar tendency for the expression of *PPARγ1* to increase during pregnancy in both genotypes, without differences between them (Figure 2A). Nevertheless, the expression of genes involved in lipid metabolism was not significantly different between PPγ2KO-P and WT-P mice (Figure 3A).

In summary, deletion of PPARγ2 is associated with a decrease in the expression of PPARγ target genes involved in lipid metabolism in subcutaneous depot, and this is exacerbated during pregnancy.

Deletion of PPARγ2 Leads to Increased Inflammation in Perigonadal but Not Subcutaneous WAT

The differential expression of lipid metabolism genes in the WAT depots of PPγ2KO-P mice prompted us to investigate whether PPARγ2 ablation was associated with depot-specific changes in WAT inflammation that could be implicated in IR.

We observed increased levels of the protease inhibitor PAI-1 in the serum of pregnant mice of both genotypes at D18, with a tendency to be higher in the PPγ2KO-P group. No differences in the levels of IL-6 and MCP-1 were observed between genotypes of pregnant mice (Table 2).

Gene expression of the macrophage markers *F4/80, Cd68* and *Cd11b* increased with pregnancy in perigonadal WAT, and this was also found in PPγ2KO-C mice relative to WT-C mice (Figure 4A). Expression of these markers and also *Tnfα* and *Mcp1* was higher in PPγ2KO-P mice than in WT-P mice, which was associated with high-level expression of the anti-apoptotic *Bcl-2*. No significant differences in expression of these genes were found in subcutaneous WAT. In the
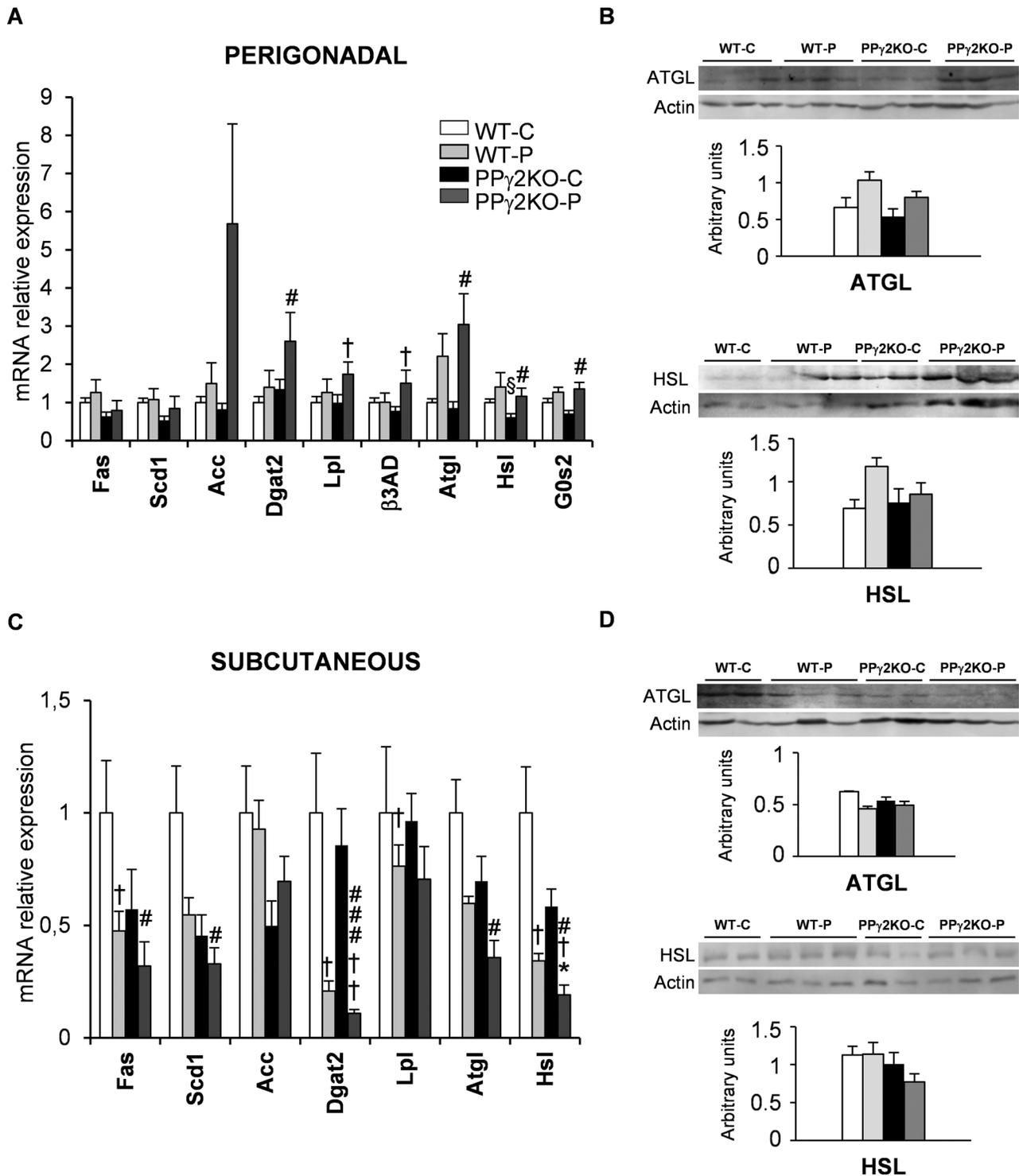
Figure 2. Expression pattern of PPARs and other adipose markers in perigonadal and subcutaneous WAT depots during pregnancy. (A and C) mRNA levels of adipogenic markers and other genes in (A) perigonadal and (C) subcutaneous fat depots from pregnant and nonpregnant WT and PPγ2KO mice. Data are expressed as mean ± SEM (n = 6–8 animals/group). (B and C) Quantification of PPARγ1 and PPARγ2 total protein expression in perigonadal (B) and subcutaneous (D) fat depots from pregnant and nonpregnant WT and PPγ2KO mice. Levels of protein were normalized to total β-actin. Data are expressed as mean ± SEM (n = 3–5 animals/group). *$p \leq .05$; *** $p \leq .001$ PPγ2KO-P versus WT-P; # $p \leq .05$; ###$p \leq .001$ PPγ2KO-P versus WT-C; † $p \leq .05$; ††† $p \leq .001$ pregnant versus non pregnant; § $p \leq .05$ PPγ2KO-C versus WT-C.

Figure 3. Role of PPARγ2 in fat storage and mobilization in perigonadal and subcutaneous WAT depots during pregnancy. (A and C) mRNA levels of lipogenic and lipolytic genes in (A) perigonadal and (C) subcutaneous fat depots from pregnant and nonpregnant WT and PPγ2KO mice. Data are expressed as mean ± SEM (n = 6–8 animals/group). Total protein quantification of lipolytic enzymes ATGL and HSL in homogenates from (B) perigonadal and (D) subcutaneous fat depots from pregnant and nonpregnant WT and PPγ2KO mice. Levels of protein were normalized to total β-actin. Data are expressed as mean ± SEM (n = 3–5 animals/group). *$p \leq .05$ PPγ2KO-P versus WT-P; #$p \leq .05$; ###$p \leq .001$ PPγ2KO-P versus WT-C; † $p \leq .05$; †† $p \leq .01$ pregnant versus non pregnant; § $p \leq .05$ PPγ2KO-C versus WT-C.

Table 2. Serum metabolic parameters measured under fed conditions on d 18 of pregnancy.

	WT-C	WT-P	PPγ2KO-C	PPγ2KO-P
Glucose (mg/dL)	144.90 ± 5.21	126.9 ± 4.93†	145.50 ± 2.52	140.90 ± 6.78
Insulin (ng/mL)	0.43 ± 0.08	0.68 ± 0.20	0.48 ± 0.05	1.17 ± 0.22†#
Adiponectin (μg/mL)	5.67 ± 1.03	4.40 ± 0.34	2.50 ± 0.37§§	1.07 ± 0.08†##*
Leptin (ng/mL)	1.12 ± 0.17	6.40 ± 1.32††	1.60 ± 0.33	5.40 ± 0.89††##
Leptin/adiponectin	-	1.44	-	6.36
Glucagon (pg/mL)	117.80 ± 16.42	124.1 ± 44.99	215.0 ± 60.87	93.75 ± 40.04
FFA (mM)	-	0.43 ± 0.07	-	0.42 ± 0.05
Fasting FFA (mM)	-	0.67 ± 0.10	-	1.03 ± 0.37
TGs (mg/dL)	87.10 ± 11.94	117.80 ± 10.24	71.00 ± 4.89	144.41 ± 26.17†#
PAI-1 (ng/mL)	3.90 ± 0.98	39.20 ± 2.42†	1.90 ± 0.30§	47.40 ± 6.35†
IL-6 (pg/mL)	-	2.20 ± 0.23	-	2.60 ± 0.22
MCP-1 (pg/mL)	-	51.00 ± 7.02	-	49.90 ± 6.82
Progesterone (ng/mL)	-	1.20 ± 0.17	-	0.50 ± 0.15**

Data are expressed as mean ± SEM (n = 6–10 animals/group). † $p \le .05$; †† $p \le .01$ pregnant versus non-pregnant, # $p \le .05$; ## $p \le .01$ PPγ2KO-P versus WT-C. §§ $p \le .01$ PPγ2KO-C versus WT-C. * $p \le .05$; ** $p \le .01$ PPγ2KO-P versus WT-P.

case of MCP-1 expression, the difference in mRNA levels was confirmed by immunohistochemistry (Figure 4B). Moreover, macrophages surrounding dying/dead adipocytes, detected as crown-like structures, were more prevalent in perigonadal WAT of PPγ2KO-P mice than WT-P mice (Figure 4B). This was associated with a phenotypic switch in WAT macrophage polarization, as indicated by higher *Cd11c* and *Il-1β* expression in the perigonadal depot of PPγ2KO-P mice than in other experimental groups. Expression of the M2 macrophage marker Ym1 was also increased in perigonadal WAT of PPγ2KO-P mice relative to WT-P mice, but not expression of *Rentla*, which was unchanged between groups. Low *Rentla* mRNA expression correlated with pregnancy in subcutaneous WAT (Figure 4A). Moreover, no differences were found in expression of a second M2 marker, *arginase 1*, which was very poorly expressed (data not shown).

Hepatic Lipotoxicity and Morphological Changes and ER Stress in the Pancreas of Pregnant PPγ2KO Mice During Gestation

An increase in liver weight in PPγ2KO-P mice (Table 1) suggested accumulation of lipids. Indeed, measurement of total lipids

in livers revealed a higher lipid content in PPγ2KO-P mice than WT-P mice (Table 1), concomitant with increased expression in the liver fatty acid uptake protein (Cd36) (Figure 5A). Expression of *PPARγ1* and *γ2* in the liver was lower during pregnancy and very low in PPγ2KO-P livers. No differences were found in the expression of other lipid metabolism genes between pregnant groups.

Given the IR detected in PPγ2KO-P mice and the altered gene expression of lipid metabolism in subcutaneous fat depots, we next examined changes in pancreas morphology and function. As expected, pancreatic islet size showed a tendency to be greater in WT-P mice than WT-C mice, but no increase in islet area was found in PPγ2KO-P mice with respect to WT-P mice (Figure 5B). Additionally, β-cells in PPγ2KO-P mice were particularly susceptible to endoplasmic reticulum (ER) stress, leading to increased perinuclear cytoplasmatic expression of C/EBP homologous protein (CHOP), accompanied by its nuclear translocation (Figure 5C).

DISCUSSION

Given the importance of WAT expansion during gestation and the central role of PPARγ in WAT function, we used the

PPγ2KO murine model to investigate the role of PPARγ2 during the last phase of pregnancy by examining gene transcriptional circuits in perigonadal and subcutaneous WAT depots. Loss of PPARγ2 intensified IR during the last term of pregnancy, and this was associated with decreased circulating adiponectin and increased body weight. The increase in IR was also associated with enhanced lipid accumulation in the liver, diminished islet expansion and increased ER stress in β-cells. Although we could not detect differences in the degree of WAT IR between PPγ2KO and WT mice during the last term of pregnancy, our data revealed significant differences in the transcriptional profile between fat depots of PPγ2KO-P mice. Accordingly, we found a decrease in the expression of genes involved in lipid metabolism in subcutaneous WAT from PPγ2KO-P and an increase in inflammation in perigonadal WAT. Thus, subcutaneous WAT function was compromised in PPγ2KO-P mice, while the homeostasis of perigonadal depots was dysregulated by decreased mass and increased inflammation.

The increased body weight of PPγ2KO-P mice is consistent with the increased liver weight, which was associated with significantly higher lipid content. Pancreas weight was also significantly increased in PPγ2KO-P mice. Differences in the weight of other tissues cannot be ruled out to explain the alteration in total body weight between PPγ2KO-P and WT-P mice. With respect to WAT depots, our results indicate less WAT expansion in PPγ2KO-P mice during gestation, as suggested by the lower weight of perigonadal fat despite higher lipid content, when compared with subcutaneous WAT. Nevertheless, it should be considered that subcutaneous tissue presented lower fat content than perigonadal fat, likely due to the increasing number of epithelial cells that would evolve from adipocytes during late pregnancy to ensure proper development of the mammary gland (22). Several studies have found lower levels of *PPARγ* in subcutaneous WAT during pregnancy
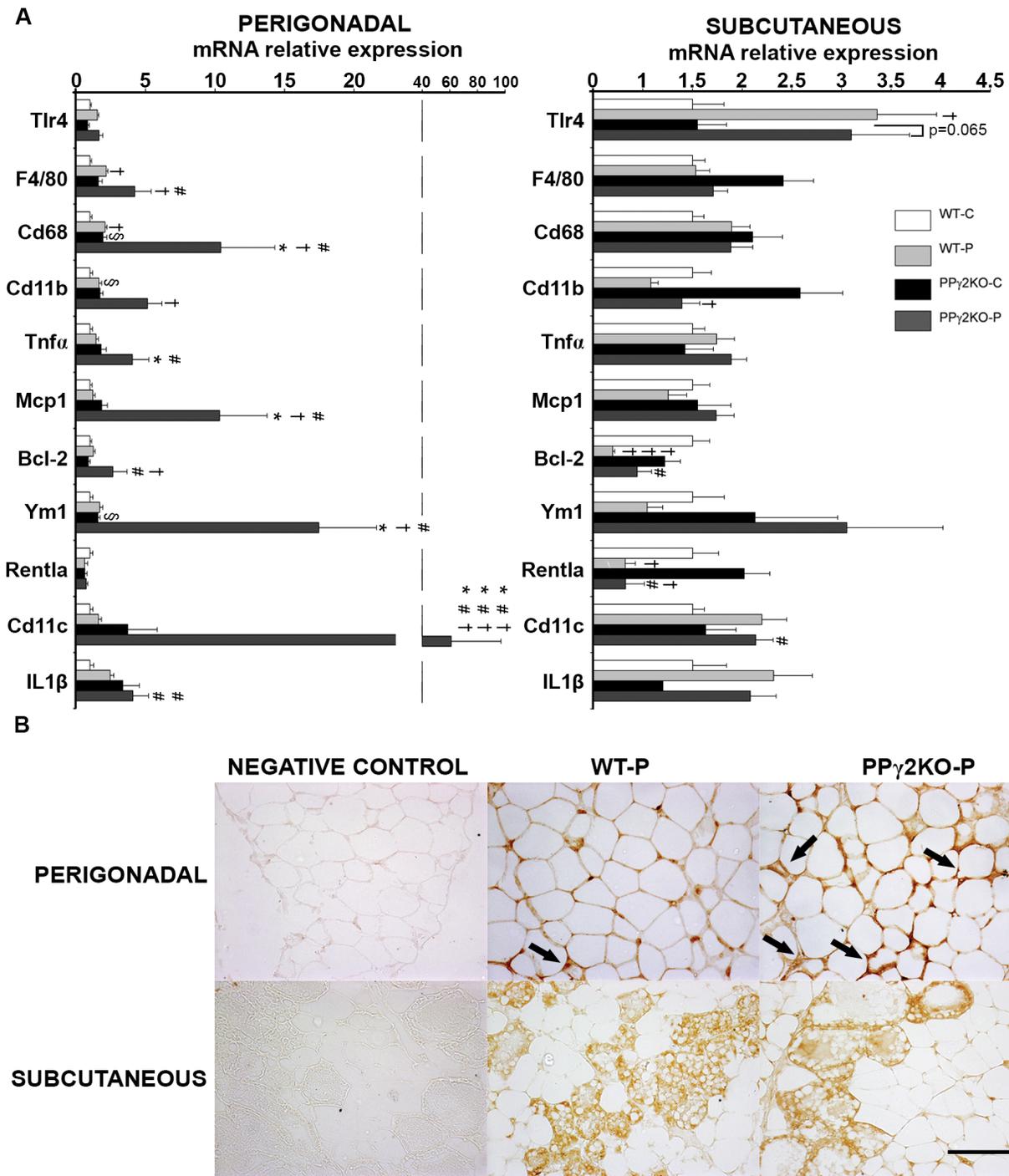
Figure 4. Increased inflammation in perigonadal but not subcutaneous WAT in pregnant mice lacking PPARγ2. (A) mRNA levels of representative inflammatory genes in perigonadal and subcutaneous fat depots from pregnant and nonpregnant WT and PPγ2KO mice. Data are expressed as mean ± SEM (n = 6–8 animals/group). † $p ≤ .05$; ††† $p ≤ .001$ pregnant versus nonpregnant; # $p ≤ .05$ ### $p ≤ .001$ PPγ2KO-P versus WT-C; * $p ≤ .05$ *** $p ≤ .001$ PPγ2KO-P versus WT-P; § $p ≤ .05$ PPγ2KO-C versus WT-C. (B) Immunohistochemical analysis of MCP-1 expression in paraffin-embedded perigonadal and subcutaneous fat depots from pregnant WT and PPγ2KO groups (n = 4 animals/group). No immunoreaction was observed in the negative control treated with PBS without primary antibody. Arrows indicate the locations of infiltrated macrophages, which form crown-like structures surrounding dead and dying adipocytes, which express MCP-1. Original magnification × 200. Scale bar: 100 μm.
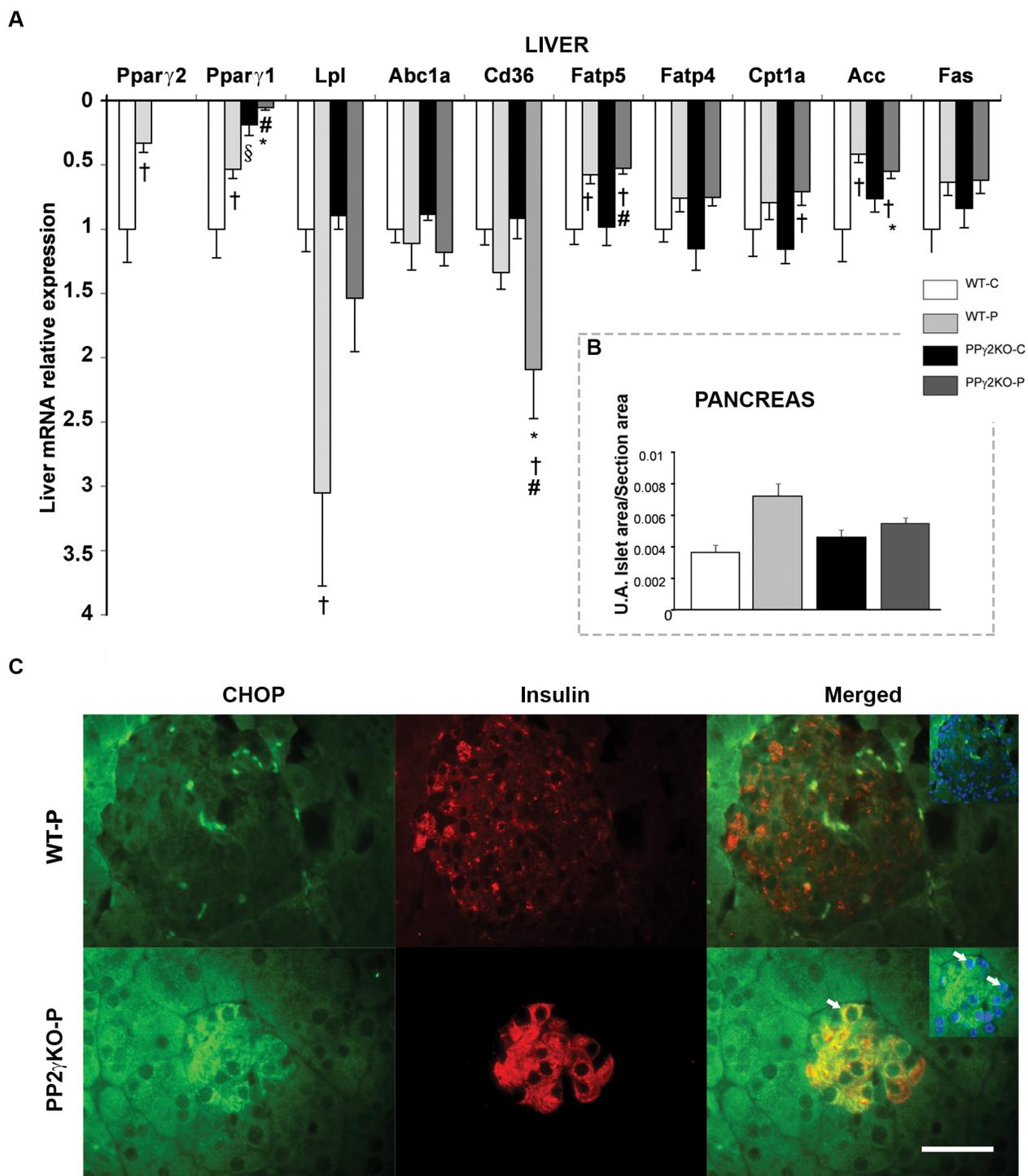
Figure 5. Expression levels of genes involved in hepatic lipid metabolism and morphological changes of the pancreas in the PPγ2KO mouse at late pregnancy. (A) mRNA levels of hepatic lipid metabolism genes in pregnant and nonpregnant WT and PPγ2KO mice (n = 6 animals/group). † $p \leq .05$ pregnant versus non pregnant; # $p \leq .05$ PPγ2KO-P versus WT-C; § $p \leq .05$ PPγ2KO-C versus WT-C; * $p \leq .05$ PPγ2KO-P versus WT-P. (B) Average area of the islets relative to total area of the analyzed pancreatic section in each group (A.U.: arbitrary units). (C) Representative images of insulin (red), CHOP (green) and nucleus (blue) immunohistochemistry in islets from pregnant WT and PPγ2KO mice (n = 4 animals/group). Arrows indicate colocalization of insulin and CHOP. Merged show original magnification × 400. Scale bar: 50 μm.

and in obese pregnant women (15,23). This could be associated with IR and a decreased capacity to store lipids. The difference in expression of both *PPARγ* isoforms in the subcutaneous depot of WT-P could indicate that, in healthy pregnancy, the decreased storage of lipids in the last phase of gestation would largely depend on declined expression of *PPARγ2* isoform in this depot.

Human adipose tissue expansion in pregnancy is impaired in GDM (24). Our results reveal a decrease in the weight of perigonadal fat in PPγ2KO-P mice, suggesting that this depot would be at the limit of its capacity of growth and likely to be dysfunctional. This would be in agreement with the hypertriglyceridemia and higher content of lipids in the liver in PPγ2KO-P mice.

A decrease in *PPARγ* expression, in both human and murine models, is associated with failure of the lipolytic process (25,26). Lipolytic gene expression was increased in the perigonadal depot of PPγ2KO-P mice, whereas it was decreased in the subcutaneous fat, suggesting that during pregnancy the subcutaneous depot is functionally compromised. In line with this notion, previous studies have demonstrated that perigonadal fat does not increase in mass and has higher lipolytic capacity than subcutaneous fat in obese pregnancy (27,28). According to our study, we speculate that increased lipolysis together with the lack of expandability could explain the decreased mass of perigonadal WAT in PPγ2KO-P mice.

The higher IR in PPγ2KO-P mice at late pregnancy was indicated by results of the ITT and also by the low level of plasma adiponectin. Adiponectin decreases during pregnancy (29–31), and we previously found that it contributes to the physiological IR characteristic of this period (3). Thus pregnancy and the dependence of *adiponectin* expression on PPARγ (11,12) may explain the significantly lower levels of *adiponectin* and the IR in PPγ2KO-P mice. The altered distribution of fat mass is another factor that could explain the low *adiponectin*

levels detected in PPγ2KO-P mice. In situations of hypoadiponectinemia in humans, redistribution of fat in different depots or in other tissues determines the existence of low levels of *adiponectin*, especially when the fat is deposited in visceral depots, liver or muscle (32–34). Furthermore, we speculate that the lack of insulin stimulation observed in muscle from PPγ2KO-P mice could be related to alterations in WAT, and could also contribute to the higher degree of peripheral IR found in these animals.

Despite the aggravated IR, we did not detect an increase in the size of islets in PPγ2KO-P mice. This failure to expand β-cell mass was associated with increased ER stress, suggesting β-cell over workload in PPγ2KO-P mice due the high rate of protein synthesis for adapting to IR and decreased expansion of islets. This pattern of ER stress has also been shown in obese patients with type 2 diabetes (35). Thus, analogous to our description under obese conditions (14), PPARγ2 could also be involved in the β-cell adaptation to IR associated with pregnancy.

The lower expandability of perigonadal tissue and increased IR would also be in agreement with the increased inflammatory signals described here in perigonadal WAT of PPγ2KO-P mice. Gestation coexists with a state of generalized mild chronic inflammation, which is characterized by increased levels of circulating inflammatory cytokines, and locally by an increase in infiltration of macrophages into adipose tissue (9,10,36–38). The inflammatory process is physiological at the end of normal pregnancy (36); however, it is pathological in pregnancy associated with obesity and GDM (10,37). Given its anatomical location close to the fetus and its higher lipolytic capacity, perigonadal WAT has been proposed as the fat depot that supplies more nutrients to the fetus (39).

We propose that PPARγ2 would be essential for WAT expansion during pregnancy as well as for the control of metabolic processes in perigonadal and subcutaneous fat depots (Figure 6).

Other studies in humans suggest that the difference between pregnant women with metabolic problems and healthy women would not be determined only by a greater amount of accumulated fat, but also by body fat distribution (28). Several published cases in pregnancy are known in relation to the possible failure of expandability of the perigonadal depot as a result of inactive PPARγ2, including one patient with WAT dysfunction associated with a dominant negative mutation in PPARγ who developed hypertriglyceridemia and severe IR during pregnancy (39,40). It can be speculated that the aggravated IR, lower perigonadal WAT expandability and higher inflammation found in our PPγ2KO mouse model during the first pregnancy would make subsequent pregnancy developments more severe.

CONCLUSION

Here we demonstrate that PPARγ2 is essential in regulating energetic metabolism during pregnancy, and our data suggest that failure in adipose tissue functionality and β-cell adaptation could severely affect metabolism in pregnancy. We show that PPARγ2 seems to be necessary to allow WAT expansion and immune and metabolic functionality of perigonadal WAT during pregnancy, to ensure the correct contribution of energy substrates for normal gestation to term.

In summary, this work highlights the importance of PPARγ2 for adipose tissue function, and specifically subcutaneous and perigonadal depots, ensuring metabolic homeostasis and averting worsening of IR during pregnancy. Further investigation should address the underlying molecular mechanisms involved in the different fat depots during gestation.
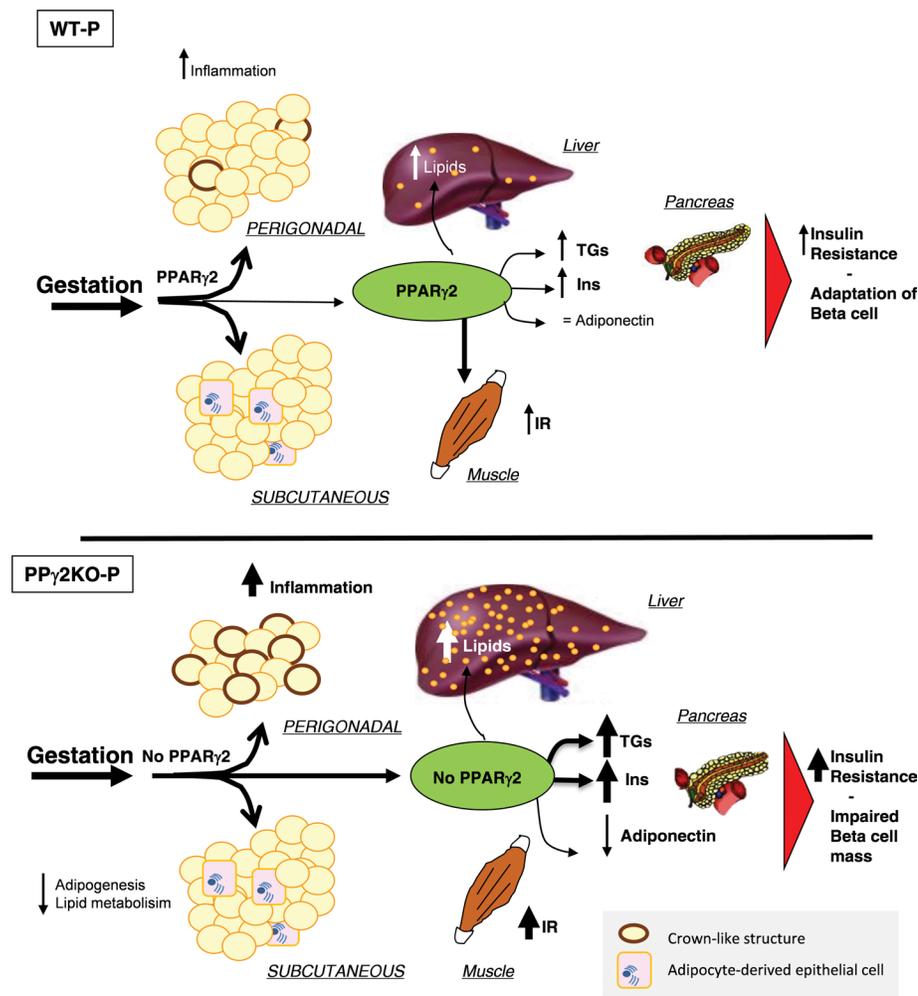
Figure 6. Role of PPARγ2 in the different adipose tissue depots during late pregnancy. Pregnant WT mice can expand both perigonadal and subcutaneous fat, inducing physiological insulin resistance and adaptation of β-cell mass. The absence of PPARγ2 in mouse perigonadal and subcutaneous fat, liver, muscle and β-cells during pregnancy results in inflammation associated with a lack of expansion of perigonadal fat, compromised subcutaneous fat and increased deposition of lipids in the liver, leading to marked peripheral insulin resistance and impaired β-cell mass. Inflammation shown as macrophages surrounding dying or dead adipocytes, detected as crown-like structures. Adipocyte-derived epithelial cells are shown in subcutaneous fat depot during pregnancy. TGs: triacylglycerides; Ins: insulin; IR: insulin resistance.

DISCLOSURE

REFERENCES

1. Ramos MP, Crespo-Solans MD, del Campo S, Cacho J, Herrera E. (2003) Fat accumulation in the rat during early pregnancy is modulated by enhanced insulin responsiveness. *Am. J. Physiol. Endocrinol. Metab.* 285(2):E318–28.

2. Colomiere M, Permezel M, Lappas M. (2010) Diabetes and obesity during pregnancy alter insulin signalling and glucose transporter expression in maternal skeletal muscle and subcutaneous adipose tissue. *J Mol. Endocrinol.* 44(4):213–23.

3. Sevillano J, de Castro J, Bocos C, Herrera E, Ramos MP. (2007) Role of insulin receptor substrate-1 serine 307 phosphorylation and adiponectin in adipose tissue insulin resistance in late pregnancy. *Endocrinology.* 148(12):5933–42.

4. Resi V, *et al.* (2012) Molecular inflammation and adipose tissue matrix remodeling precede physiological adaptations to pregnancy. *Am. J. Physiol. Endocrinol. Metab.* 303(7):E832–40.

5. Barbarroja N, *et al.* (2010) The obese healthy paradox: is inflammation the answer? *Biochem. J.* 430(1):141–49.

6. Garg A, Misra A. (2004) Lipodystrophies: rare disorders causing metabolic syndrome. *Endocrinol Metab. Clin. North. Am.* 33(2):305–31.

7. Bluher M. (2005) Transgenic animal models for the study of adipose tissue biology. *Best Pract. Res. Clin. Endocrinol. Metab.* 19(4):605–23.

8. Gustafson B, Hammarstedt A, Hedjazifar S, Smith U. (2013) Restricted adipogenesis in hypertrophic obesity: the role of WISP2, WNT, and BMP4. *Diabetes.* 62(9):2997–3004.

9. De Castro J, *et al.* (2011) Implication of low level inflammation in the insulin resistance of adipose tissue at late pregnancy. *Endocrinology.* 152(11):4094–4105.

10. Harlev A, *et al.* (2014) Macrophage infiltration and stress-signaling in omental and subcutaneous adipose tissue in diabetic pregnancies. *J. Matern. Fetal Neonatal. Med.* 27(12):1189–94.

11. Medina-Gomez G, *et al.* (2005) The link between nutritional status and insulin sensitivity is dependent on the adipocyte-specific peroxisome proliferator-activated receptor-gamma2 isoform. *Diabetes.* 54(6):1706–16.

12. Medina-Gomez G, *et al.* (2007) PPAR gamma 2 prevents lipotoxity by controlling adipose tissue expandability and peripheral lipid metabolism. *PLoS Genet.* 3(4):e64.

13. Medina-Gomez G, *et al.* (2009) Adaptation and failure of pancreatic beta cells in murine models with different degrees of metabolic syndrome. *Dis. Model Mech.* 2(11–12):582–92.

14. Vivas Y, *et al.* (2011) Early peroxisome proliferator-activated receptor gamma regulated genes involved in expansion of pancreatic beta cell mass. *BMC Med. Genomics.* 4:86.

15. Catalano PM, *et al.* (2002) Downregulated IRS-1 and PPARgamma in obese women with gestational diabetes: relationship to FFA during pregnancy. *Am. J. Physiol. Endocrinol. Metab.* 282(3):E522–33.

16. Herrera E (2000) Metabolic adaptations in pregnancy and their implications for the availability of substrates to the fetus. *Eur. J. Clin. Nutr.* 54 Suppl 1:S47–51.

17. Martinez-Garcia C, *et al.* (2012) Accelerated renal disease is associated with the development of

metabolic syndrome in a glucolipotoxic mouse model. *Dis. Model Mech.* 5(5):636–48.

18. Pfaffl MW, Tichopad A, Prgomet C, Neuvians TP. (2004) Determination of stable housekeeping genes, differentially regulated target genes and sample integrity: BestKeeper—Excel-based tool using pair-wise correlations. *Biotechnol. Lett.* 26(6):509–15.

19. Folch J, Lees M, Sloane Stanley GH. (1957) A simple method for the isolation and purification of total lipides from animal tissues. *J. Biol. Chem.* 226(1):497–509.

20. Herrera E, Ayanz A (1972) Calculation of lipolysis and esterification from glycerol metabolism in rat adipose tissue. *J. Lipid Res.* 13(6):802–09.

21. Lopez-Jaramillo P, *et al.* (2014) The role of leptin/adiponectin ratio in metabolic syndrome and diabetes. *Horm. Mol. Biol. Clin. Investig.* 18(1):37–45.

22. Cinti S. (2012) The adipose organ at a glance. *Dis. Model Mech.* 5(5):588–94.

23. Lappas M. (2014) Effect of pre-existing maternal obesity, gestational diabetes and adipokines on the expression of genes involved in lipid metabolism in adipose tissue. *Metabolism.* 63(2):250–62.

24. Rojas-Rodriguez R, *et al.* (2015) Human adipose tissue expansion in pregnancy is impaired in gestational diabetes mellitus. *Diabetologia.* 58(9):2106–14.

25. Rodriguez-Cuenca S, Carobbio S, Vidal-Puig A. (2012) Ablation of Pparg2 impairs lipolysis and reveals murine strain differences in lipolytic responses. *FASEB J.* 26(5):1835–44.

26. Rodriguez-Cuenca S, *et al.* (2012) Peroxisome proliferator-activated receptor gamma-dependent regulation of lipolytic nodes and metabolic flexibility. *Mol. Cell. Biol.* 32(8):1555–65.

27. Pujol E, *et al.* (2003) Gender- and site-related effects on lipolytic capacity of rat white adipose tissue. *Cell Mol. Life Sci.* 60(9):1982–89.

28. Jarvie E, *et al.* (2010) Lipotoxicity in obese pregnancy and its potential role in adverse pregnancy outcome and obesity in the offspring. *Clin. Sci. (Lond.)* 119(3):123–29.

29. Combs TP, *et al.* (2003) Sexual differentiation, pregnancy, calorie restriction, and aging affect the adipocyte-specific secretory protein adiponectin. *Diabetes.* 52(2):268–76.

30. Catalano PM, *et al.* (2006) Adiponectin in human pregnancy: implications for regulation of glucose and lipid metabolism. *Diabetologia.* 49(7):1677–85.

31. Barbour LA, *et al.* (2007) Cellular mechanisms for insulin resistance in normal pregnancy and gestational diabetes. *Diabetes Care.* 30 Suppl 2:S112–19.

32. Thamer C, *et al.* (2002) Relationship between serum adiponectin concentration and intramyocellular lipid stores in humans. *Horm. Metab. Res.* 34(11–12):646–49.

33. Reeds DN, *et al.* (2006) Alterations in liver, muscle, and adipose tissue insulin sensitivity in men with HIV infection and dyslipidemia. *Am. J. Physiol. Endocrinol. Metab.* 290(1):E47–E53.

34. Bugianesi E, *et al.* (2005) Plasma adiponectin in nonalcoholic fatty liver is related to hepatic insulin resistance and hepatic fat content, not to liver disease severity. *J. Clin. Endocrinol. Metab.* 90(6):3498–3504.

35. Huang C, *et al.* (2007) High expression rates of human islet amyloid polypeptide induce endoplasmic reticulum stress mediated beta-cell apoptosis, a characteristic of humans with type 2 but not type 1 diabetes. *Diabetes.* 56(8):2016–27.

36. Zhang L, *et al.* (2011) The inflammatory changes of adipose tissue in late pregnant mice. *J Mol. Endocrinol.* 47(2):157–65.

37. Basu S, *et al.* (2011) Pregravid obesity associates with increased maternal endotoxemia and metabolic inflammation. *Obesity (Silver Spring).* 19(3):476–82.

38. Lappas M, Permezel M, Rice GE. (2004) Release of proinflammatory cytokines and 8-isoprostane from placenta, adipose tissue, and skeletal muscle from normal pregnant women and women with gestational diabetes mellitus. *J. Clin. Endocrinol. Metab.* 89(11):5627–33.

39. Pujol E, Proenza A, Llado I, Roca P. (2005) Pregnancy effects on rat adipose tissue lipolytic capacity are dependent on anatomical location. *Cell Physiol. Biochem.* 16(4–6):229–36.

40. Morse AN, Whitaker MD. (2000) Successful pregnancy in a woman with lipoatrophic diabetes mellitus. A case report. *J. Reprod. Med.* 45(10):850–52.

41. Madhra M, Noh RM, Zammitt NN, Patrick AW, Love CDB. (2012) A complicated pregnancy in a patient with lipodystrophic diabetes attributable to a peroxisome proliferator-activated receptor gamma (PPARG) mutation. *Diabet. Med.* 29(10):e398–401.